

Article

Effects of Annealing Temperature on Optical Band Gap of Sol-gel Tungsten Trioxide Films

Guanguang Zhang, Kuankuan Lu, Xiaochen Zhang, Weijian Yuan, Muyang Shi, Honglong Ning * , Ruiqiang Tao, Xianzhe Liu, Rihui Yao *  and Junbiao Peng

Institute of Polymer Optoelectronic Materials and Devices, State Key Laboratory of Luminescent Materials and Devices, South China University of Technology, Guangzhou 510640, China; msgg-zhang@mail.scut.edu.cn (G.Z.); mskk-lu@mail.scut.edu.cn (K.L.); mszhang_xc@mail.scut.edu.cn (X.Z.); 201430320366@mail.scut.edu.cn (W.Y.); 201430320229@mail.scut.edu.cn (M.S.); 201510102158@mail.scut.edu.cn (R.T.); msliuxianzhe@mail.scut.edu.cn (X.L.); psjbpeng@scut.edu.cn (J.P.)
* Correspondence: ninghl@scut.edu.cn (H.N.); yaorihui@scut.edu.cn (R.Y.); Tel.: +86-20-8711-4525 (H.N.)

Received: 6 July 2018; Accepted: 25 July 2018; Published: 30 July 2018



Abstract: Tungsten trioxide (WO_3) is a wide band gap semiconductor material that is used as an important electrochromic layer in electrochromic devices. In this work, the effects of the annealing temperature on the optical band gap of sol-gel WO_3 films were investigated. X-ray Diffraction (XRD) showed that WO_3 films were amorphous after being annealed at 100 °C, 200 °C and 300 °C, respectively, but became crystallized at 400 °C and 500 °C. An atomic force microscope (AFM) showed that the crystalline WO_3 films were rougher than the amorphous WO_3 films (annealed at 200 °C and 300 °C). An ultraviolet spectrophotometer showed that the optical band gap of the WO_3 films decreased from 3.62 eV to 3.30 eV with the increase in the annealing temperature. When the Li^+ was injected into WO_3 film in the electrochromic reaction, the optical band gap of the WO_3 films decreased. The correlation between the optical band gap and the electrical properties of the WO_3 films was found in the electrochromic test by analyzing the change in the response time and the current density. The decrease in the optical band gap demonstrates that the conductivity increases with the corresponding increase in the annealing temperature.

Keywords: optical band gap; tungsten trioxide film; annealing temperature; electrochromism

1. Introduction

Tungsten trioxide (WO_3) is an important indirect band gap semiconductor material [1]. It is used as a functional layer in the applications of gas sensors [2], photocatalysis [3], solar cells [4], water splitting [5] and electrochromism [6]. Electrochromic devices, such as smart windows [7], can meet the market demand of energy-saving devices. Since WO_3 's electrochromic properties were found, researchers have widely studied WO_3 -based electrochromic thin films and device applications [8].

There are various choices for preparing WO_3 films with the development of thin film technology. These include sputtering [9], chemical vapor deposition [10], vacuum evaporation [11], and sol-gel [12], among others. Currently, magnetron sputtering is a commercial technology that is used to prepare WO_3 films due to its uniformity of film and reliability. However, the high cost issue and problems in preparing large-size devices cannot be ignored. The sol-gel method is a feasible technology for reducing the cost even, though there are still some problems at the present stage, such as film inhomogeneity and poor process repeatability, among others. With the development of new sol-gel techniques, such as inkjet printing [13], sol-gel technology is promising for commercial applications in the future.

The optical and electrical properties of WO_3 film are related to the parameters of the sol-gel technique, such as the solvent [14], precursor [15] and annealing temperature [16], among others.

In previous work, there was a significant difference in the band gap of the WO_3 films obtained using different processes [17,18]. Therefore, it is worthwhile to launch further investigations into the relationship between band gap and the optical and electrical properties of WO_3 films, especially in regards to electrochromic properties. In this paper, we conducted a study on the optical band gap of WO_3 films with different annealing temperatures. The crystallinity, response time morphology and conductivity were also analyzed together. A correlation between the optical band gap and the electrical properties (conductivity) was found.

2. Materials and Methods

Tungsten powder (W, 99.5% metals basis, Macklin Biochemical Co. Ltd, Shanghai, China) and hydrogen peroxide (H_2O_2 , Hydrogen peroxide 30%, Guangzhou chemical reagent factory, Guangzhou, China) were mixed in a beaker with a water bath at 25 °C. After the reaction finished, an evaporative concentration treatment (at 150 °C) was conducted to remove the surplus H_2O_2 . Finally, an appropriate anhydrous ethanol was added into the concentrated solution and the mixed solution was sealed and stirred for 3 h at 70 °C to obtain the sol-gel. A spin coating technique was used to prepare the WO_3 films (around 80 nm) on the indium tin oxide (ITO) glass. The thickness of the WO_3 film was optimized and controlled by the concentration of solution and spin coating parameters and it had an important influence on the electrochromic transmittance modulation ability [19]. In this work, the annealing temperature was focused on and other unrelated variables (sol concentration, spin coating parameters, substrate, electrolyte, etc.) were controlled. These as-deposited films were annealed at 100 °C, 200 °C, 300 °C, 400 °C and 500 °C for 60 min, respectively.

The crystallization of the film was analyzed by X-ray Diffraction (XRD, PANalytical Empyrean DY1577, PANalytical, Almelo, The Netherlands). The surface morphology was measured by atomic force microscopy (AFM, Being Nano-Instruments BY3000 Being Nano-Instruments, Beijing, China). The electrochromic test was performed using 0.8 mol/L of lithium perchlorate/propylene carbonate (LiClO_4/PC) electrolyte and an electrode gap (~1 mm). The transmission spectra were measured by an Ultraviolet spectrophotometer (SHIMADZU UV2600, SHIMADZU, Tokyo, Japan), with ITO glass (Optical band gap: >4 eV) acting as a blank. The current of the electrochromic test was recorded by an electrochemical workstation (CH Instruments CHI600E, CH Instruments, Shanghai, China). The relationship between the change of transmittance and the time was measured by a micro-spectrometer (Morpho PG2000, Morpho, Shanghai, China), with ITO glass acting as a blank.

3. Results and Discussions

Figure 1 illustrates the X-ray patterns of the WO_3 films that were annealed at different temperatures. The crystalline structures of these films were further analyzed using Jade 6.0 and PDF#30-1387 and PDF#41-0905. In Figure 1a, there are diffraction peaks of WO_3 at the patterns of the WO_3 films annealed at 400 °C and 500 °C, which demonstrate that these films transformed from amorphous to crystalline when the annealing temperature is higher than 400 °C. Furthermore, the change of crystalline structure was analyzed in Figure 1b. The characteristic diffraction peaks of WO_3 films (400 °C) indicate that the WO_3 films initially transform from an amorphous to a monoclinic structure. When the annealing temperature reached 500 °C, there was only one diffraction peak of the WO_3 film in the range of 2θ (22° to 26°), which demonstrated that the monoclinic structure of the WO_3 films turned into a cubic structure. Strictly speaking, the stoichiometric ratio of tungsten and oxygen was not fully satisfied with 1:3. Therefore, there was an oxygen vacancy which influenced the optical and electrical properties of WO_3 films [20].

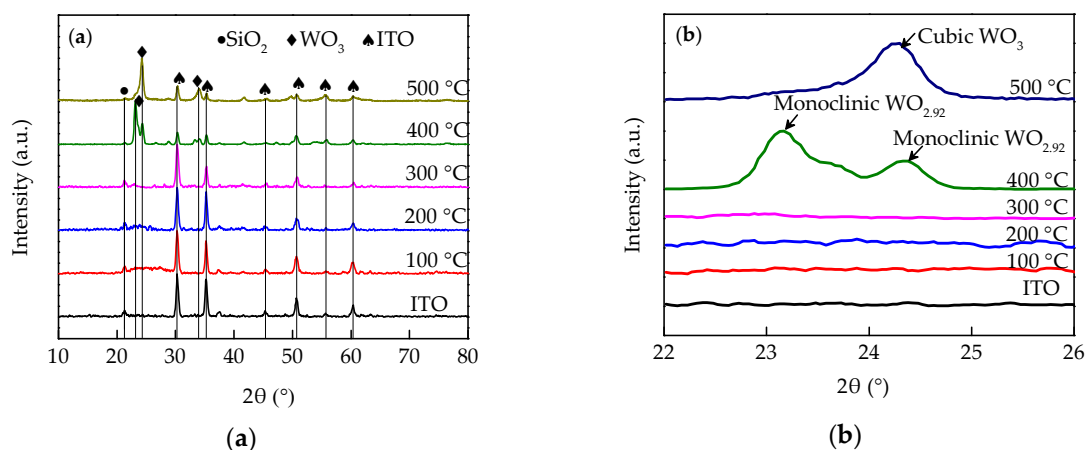


Figure 1. X-ray patterns of WO₃ films annealed at different temperature. (a) The XRD patterns in a large range of 2θ (10° to 80°); (b) The XRD patterns in a small range of 2θ (22° to 26°). The amorphous WO₃ transformed into monoclinic structure and cubic structure at 400°C and 500°C , respectively.

The surface morphology of these films was measured by AFM and the results are shown in Figure 2. Figure 2f shows a comparison of the roughness of these films at different annealing temperatures. The surface of the WO₃ film that was annealed at 100°C is rougher than other films, which is confirmed by Figure 2a and its roughness. In this work, the solvent of sol was ethanol and water, which has a boiling point of around 80°C . The 100°C annealing treatment can remove the solvent, but it is not enough to remove the bound water in the tungsten acid [21]. In addition, solvent evaporation can cause defects in the surface, such as pores [22], and there is not enough energy to reduce these defects during annealing treatment. Therefore, among these samples, the WO₃ film annealed at 100°C had the highest roughness.

The roughness of the films annealed at 200°C and 300°C was around 1.9 nm, which is less than that of the films (around 3.3 nm) annealed at 400°C and 500°C . This demonstrated that the crystalline film was rougher than the amorphous film because of its grain growth at a high temperature. The change in roughness indirectly revealed that the change in the WO₃ film composition and crystalline structure was due to the increase in the annealing temperature, which is consistent with the results of XRD.

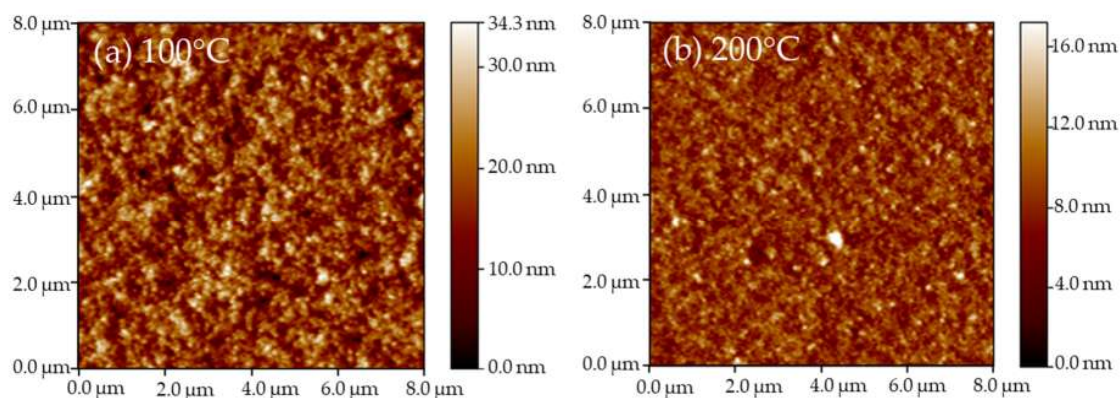


Figure 2. Cont.

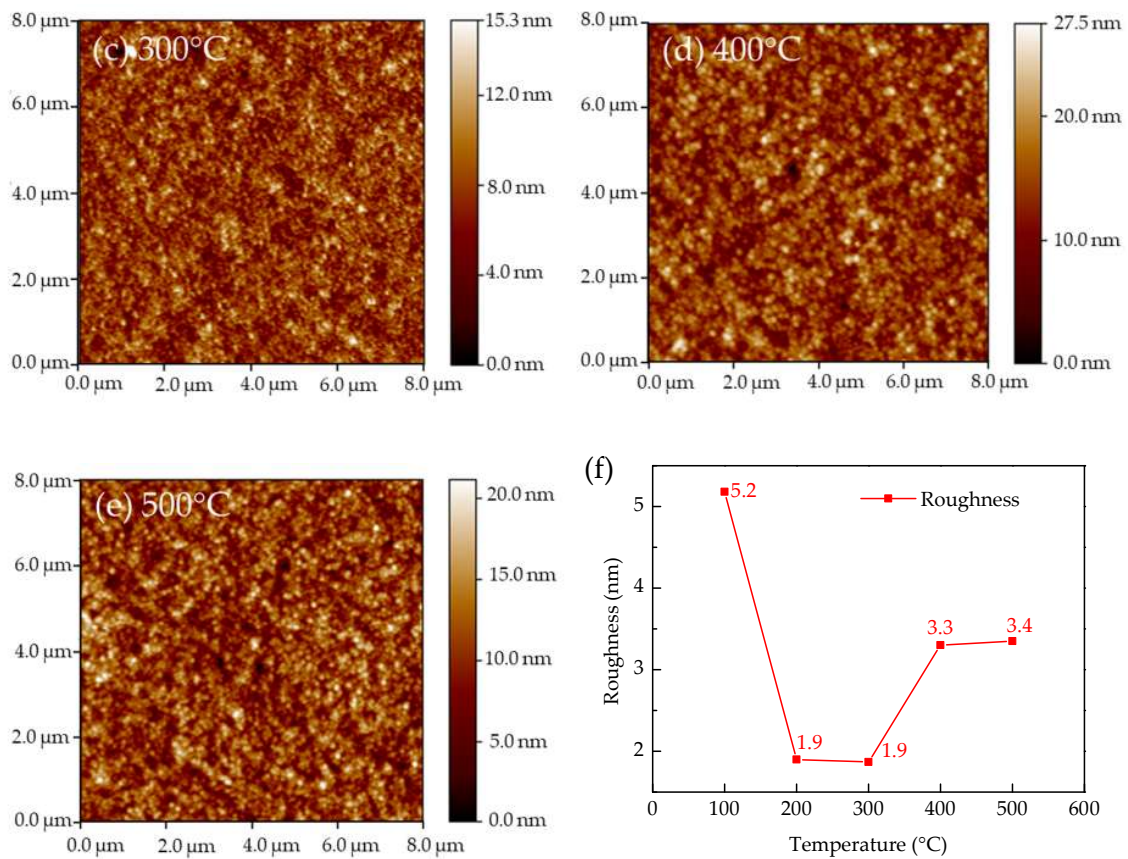


Figure 2. The atomic force microscope (AFM) images 8000 nm × 8000 nm and the roughness of WO₃ films. (a) 100 °C; (b) 200 °C; (c) 300 °C; (d) 400 °C; (e) 500 °C; (f) the roughness of WO₃ films, which are read by the support software of AFM.

The band gap of WO₃ film can be measured and analyzed by an ultraviolet spectrophotometer. The optical band gap is distinguished from the band gap measured by other methods. According to Equation (1), the optical band gap can be calculated [23].

$$\alpha h\nu = A(h\nu - E_g)^n \tag{1}$$

where α is the absorption coefficient, which can be measured by the ultraviolet spectrophotometer; h is the Planck constant; ν is the light frequency; A is a proportionality constant; E_g is the optical band gap; and n is a number which is 1/2 for the direct band gap semiconductor and 2 for the indirect band gap semiconductor. In this work, n is 2 because the WO₃ was an indirect band gap semiconductor.

To further investigate the electrochromic effects on the optical band gap of WO₃ film, the optical band gap of WO₃ film in a bleached state and colored state were analyzed. Electrochromism involves an electrochemical reaction, as shown in Equation (2) [24]:



At its bleached state, the WO₃ film is colorless. When both Li⁺ and the electron are injected into the WO₃ film under an applied voltage, the bleached state of WO₃ turns into a colored state due to the generation of blue Li_xWO₃.

Figure 3a–e illustrates the curves of $(\alpha h\nu)^{1/2}$ versus the photon energy $h\nu$, which are calculated using the transmission spectra of the WO₃ films in the colored state and the bleached state. E_g can be extracted through the onset of the optical transitions of the WO₃ films near the band edge, which is

equal to the value of the fitting line intercepts. Figure 3f shows a comparison of the optical band gap value of the WO₃ film that were annealed at different temperatures and electrochromic state (colored and bleached) and it indicates that the E_g of bleached WO₃ films decreases from 3.58 eV to 3.3 eV as the annealing temperature increases. Similarly, the E_g of the colored WO₃ film tends to decrease with an increased annealing temperature. In addition, the E_g of all the colored WO₃ films was less than that of their respective bleached WO₃ films.

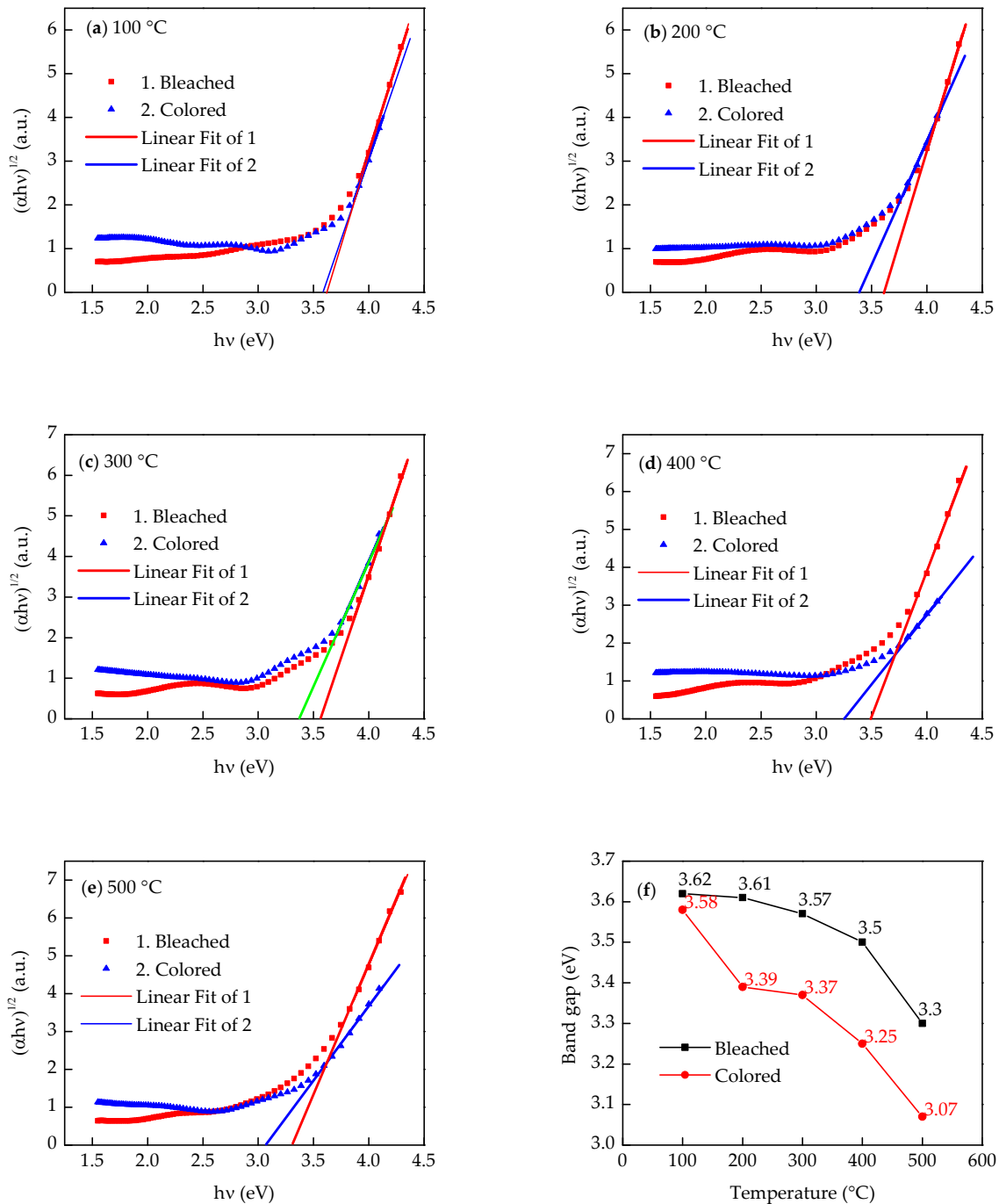


Figure 3. Optical band gap energy of WO₃ films in a colored state and bleached state. (a) 100 °C; (b) 200 °C; (c) 300 °C; (d) 400 °C; (e) 500 °C; and (f) a comparison of optical band gap energy of WO₃ films annealed at different temperature and electrochromic state (colored and bleached).

As for E_g , which decreased when the annealing temperature increased, a reasonable explanation was that as the annealing temperature increased, the oxygen vacancies increased, which may have provided free electrons and enhanced the conductivity of the WO_3 films [25].

To further investigate the relationship between E_g , conductivity, and electrochromic response time, an electrochromic test was conducted. Figure 4a,b illustrates the current density of the different WO_3 films and the change of transmittance (at 600 nm) under ± 2.5 V voltage, respectively. The peak current density of these films in the coloring process increased when the annealing temperature increased (an increase from 2.6 mA/cm² at 100 °C to 16.1 mA/cm² at 500 °C). This indicated that the conductivity enhanced with the increase in the annealing temperature. Similarly, the peak current density of these films in the bleaching process shows a similar change (increase from 11.0 mA/cm² at 100 °C to 22.2 mA/cm² at 500 °C). These were attributed to the decrease of E_g and the increase of free electrons. In addition, Figure 4a illustrates that the peak current density of the bleaching process was larger than that of coloring process, which results from the good conductivity of Li_xWO_3 [26]. This is related to the decrease of E_g after WO_3 film coloring.

Figure 4b illustrates an intuitive change of transmittance response curves. The response time is defined by the time corresponding to 90% of the total transmittance change. Figure 5 shows a specific comparison of the response time in the electrochromic test. The curve of the bleaching response time in Figure 5 shows that the bleaching response time increases from 1.2 s to 22.7 s, when the annealing temperature increased. In the bleaching process, the applied voltage drop is mainly across the electrolyte and the Li_xWO_3 layer. The extraction of Li^+ depends largely on the voltage across the Li_xWO_3 layer [27]. The E_g of the WO_3 film at the colored state reduced with the increase in the annealing temperature, which was attributed to the increase in the number of free electrons. In other words, the conductivity enhanced with the increase in annealing temperature. Therefore, the voltage across the Li_xWO_3 layer reduced with the increase in annealing temperature, which resulted in the increase of the bleaching response time. However, there was no similar trend in the coloring response time. The influence factors are not only the conductivity of the WO_3 film, but also the interface barrier of electrolyte-film [28]. The coloring response time increased when the WO_3 film changed from amorphous into crystalline, which resulted from the decrease in the voltage drop at the WO_3 layers, due to the increase in the conductivity. The band gap mainly influenced the transmission of the electrons, but the transmission of Li^+ depended more on the structure of films (such as crystallinity, morphology, etc.) [29].

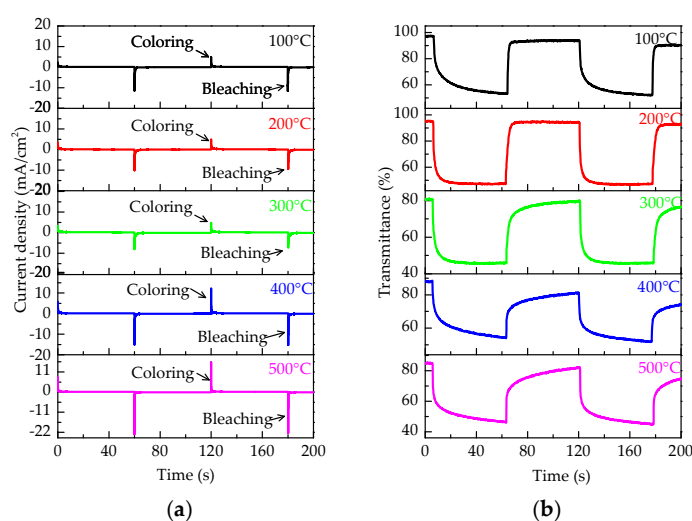


Figure 4. (a) Current change of WO_3 films at different annealing temperature. The applied voltage was ± 2.5 V and the WO_3 films were placed in the cathode; (b) change of transmittance (at 600 nm) of WO_3 films at different annealing temperature.

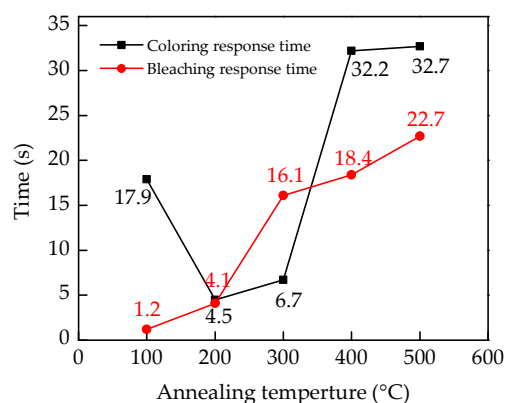


Figure 5. The curves of coloring and bleaching response time versus annealing temperature. The time corresponding to 90% of the total transmittance change is defined as the electrochromic response time.

4. Conclusions

The effects of the annealing temperature on the E_g of the WO_3 films were investigated. When the annealing temperature was higher than 400 °C, the crystalline structure of the WO_3 film changed from amorphous to monoclinic (400 °C), and then to cubic (500 °C). The E_g of the WO_3 films decreased from 3.62 eV to 3.30 eV when the annealing temperature was increased. In addition, the E_g of the colored WO_3 films was less than that of the bleached WO_3 films. The relationship between the E_g , conductivity, and electrochromic response time of the WO_3 film with different annealing temperatures demonstrates that the conductivity of the WO_3 film enhanced with the decrease in E_g , while the high conductivity increased the electrochromic response time.

Author Contributions: Conceptualization, G.Z.; Data curation, G.Z., K.L., W.Y., M.S. and X.L.; Formal analysis, G.Z., K.L., W.Y., R.T. and X.L.; Funding acquisition, H.N. and R.Y.; Investigation, X.Z. and M.S.; Methodology, X.Z., R.T. and X.L.; Project administration, H.N., R.Y. and J.P.; Supervision, H.N.; Writing—original draft, G.Z.; Writing—review & editing, K.L., H.N., R.T., X.L., R.Y. and J.P.

Acknowledgments: This work was supported by National Natural Science Foundation of China (Grant.51771074, 51521002 and U1601651), National Key R&D Program of China (No.2016YFB0401504 and 2016YFF0203600), National Key Basic Research and Development Program of China (973 program, Grant No.2015CB655004) Founded by Ministry of Science and Technology (MOST), Guangdong Natural Science Foundation (No.2016A030313459 and 2017A030310028), Guangdong Science and Technology Project (No.2016B090907001, 2016A040403037, 2016B090906002, 2017B090907016 and 2017A050503002), Guangzhou Science and Technology Project (201804020033).

Conflicts of Interest: The authors declare no conflicts of interest.

References

- Hill, J.C.; Choi, K.S. Effect of electrolytes on the selectivity and stability of n-type WO_3 photoelectrodes for use in solar water oxidation. *J. Phys. Chem. C* **2012**, *116*, 7612–7620. [[CrossRef](#)]
- Leidinger, M.; Huotari, J.; Sauerwald, T.; Lappalainen, J.; Schütze, A. Selective detection of naphthalene with nanostructured WO_3 gas sensors prepared by pulsed laser deposition. *J. Sens. Sens. Syst.* **2016**, *5*, 147–156. [[CrossRef](#)]
- Sotelo-Vazquez, C.; Quesada-Cabrera, R.; Ling, M.; Scanlon, D.O.; Kafizas, A.; Thakur, P.K.; Lee, T.L.; Taylor, A.; Watson, G.W.; Palgrave, R.G. Photocatalysis: Evidence and effect of photogenerated charge transfer for enhanced photocatalysis in WO_3/TiO_2 heterojunction films: A computational and experimental study. *Adv. Funct. Mater.* **2017**, *27*, 1605413. [[CrossRef](#)]
- Hara, K.; Zhao, Z.G.; Cui, Y.; Miyauchi, M.; Miyashita, M.; Mori, S. Nanocrystalline electrodes based on nanoporous-walled WO_3 nanotubes for organic-dye-sensitized solar cells. *Langmuir* **2011**, *27*, 12730–12736. [[CrossRef](#)] [[PubMed](#)]
- Wang, F.; Valentin, C.D.; Pacchioni, G. Doping of WO_3 for photocatalytic water splitting: Hints from density functional theory. *J. Phys. Chem. C* **2012**, *116*, 8901–8909. [[CrossRef](#)]

6. Cai, G.; Cui, M.; Kumar, V.; Darmawan, P.; Wang, J.; Wang, X.; Eh, L.S.; Qian, K.; Lee, P.S. Ultra large optical modulation of electrochromic porous WO₃ film and the local monitoring of redox activity. *Chem. Sci.* **2016**, *7*, 1373–1382. [[CrossRef](#)] [[PubMed](#)]
7. Yang, W.; Runnerstrom, E.L.; Milliron, D.J. Switchable materials for smart windows. *Annu. Rev. Chem. Biomol. Eng.* **2016**, *7*, 283–304.
8. Granqvist, C.G. Electrochromic tungsten oxide films: Review of progress 1993–1998. *Sol. Energy Mat. Sol. Cells* **2000**, *60*, 201–262. [[CrossRef](#)]
9. Lemire, C.; Lollman, D.B.B.; Mohammad, A.A.; Gillet, E.; Aguir, K. Reactive R.F. magnetron sputtering deposition of WO₃ thin films. *Sens. Actuators B Chem.* **2002**, *84*, 43–48. [[CrossRef](#)]
10. Davazoglou, D.; Leveque, G.; Donnadieu, A. Study on the optical and electrochromic properties of polycrystalline WO₃ thin films prepared by CVD. *Sol. Energy Mater.* **1988**, *17*, 379–390. [[CrossRef](#)]
11. Reichman, B.; Bard, A.J. The Electrochromic process at WO₃ electrodes prepared by vacuum evaporation and anodic oxidation of W. *J. Electrochem. Soc.* **2016**, *126*, 583–591. [[CrossRef](#)]
12. Zayim, E.O. Optical and electrochromic properties of sol-gel made anti-reflective WO₃-TiO₂ films. *Sol. Energy Mater. Sol. Cells* **2005**, *87*, 695–703. [[CrossRef](#)]
13. Wojcik, P.; Cruz, A.; Santos, L.; Pereira, L.; Martins, R.; Fortunato, E. Microstructure control of dual-phase inkjet-printed a-WO₃/TiO₂/WO_x films for high-performance electrochromic applications. *J. Mater. Chem.* **2012**, *22*, 13268–13278. [[CrossRef](#)]
14. Santos, L.; Wojcik, P.; Pinto, J.V.; Elangovan, E.; Viegas, J.; Pereira, L.; Martins, R.; Fortunato, E. Structure and morphologic influence of WO₃ nanoparticles on the electrochromic performance of dual-phase a-WO₃/WO₃ inkjet printed films. *Adv. Electron. Mater.* **2015**, *1*, 1–2. [[CrossRef](#)]
15. Mukherjee, R.; Sahay, P.P. Effect of precursors on the microstructural, optical, electrical and electrochromic properties of WO₃ nanocrystalline thin films. *J. Mater. Sci-Mater. Electron.* **2015**, *26*, 1–13. [[CrossRef](#)]
16. Chai, Y.N.; Razak, K.A.; Lockman, Z. Effect of annealing on acid-treated WO₃-H₂O nanoplates and their electrochromic properties. *Electrochimica Acta* **2015**, *178*, 673–681.
17. Gonzalez-Borrero, P.P.; Sato, F.; Medina, A.N.; Baesso, M.L.; Bento, A.C.; Baldissera, G.; Persson, C.; Niklasson, G.A.; Granqvist, C.G.; Silva, A.J.D. Optical band-gap determination of nanostructured WO₃ film. *Appl. Phys. Lett.* **2010**, *96*, 201. [[CrossRef](#)]
18. Vemuri, R.S.; Engelhard, M.H.; Ramana, C.V. Correlation between surface chemistry, density, and band gap in nanocrystalline WO₃ thin films. *ACS Appl. Mater. Interfaces* **2012**, *4*, 1371–1377. [[CrossRef](#)] [[PubMed](#)]
19. Min, H.K.; Choi, H.W.; Kim, K.H. Thickness dependence of WO_{3-x} thin films for electrochromic device application. *Mol. Cryst. Liquid Cryst.* **2014**, *598*, 54–61.
20. Arfaoui, A.; Ouni, B.; Touihri, S.; Mannoubi, T. Investigation into the optoelectrical properties of tungsten oxide thin films annealed in an oxygen air. *Mater. Res. Bull.* **2014**, *60*, 719–729. [[CrossRef](#)]
21. Szilágyi, I.M.; Santala, E.; Heikkilä, M.; Kemell, M.; Nikitin, T.; Khriachtchev, L.; Räsänen, M.; Ritala, M.; Leskelä, M. Thermal study on electrospun polyvinylpyrrolidone/ammonium metatungstate nanofibers: Optimising the annealing conditions for obtaining WO₃ nanofibers. *J. Therm. Anal. Calorim.* **2011**, *105*, 73. [[CrossRef](#)]
22. Badilescu, S.; Ashrit, P.V. Study of sol-gel prepared nanostructured WO₃ thin films and composites for electrochromic applications. *Solid State Ion.* **2003**, *158*, 187–197. [[CrossRef](#)]
23. Zou, Y.S.; Zhang, Y.C.; Lou, D.; Wang, H.P.; Gu, L.; Dong, Y.H.; Dou, K.; Song, X.F.; Zeng, H.B. Structural and optical properties of WO₃ films deposited by pulsed laser deposition. *J. Alloy Compd.* **2014**, *583*, 465–470. [[CrossRef](#)]
24. Haro-Poniatowski, E.; Jouanne, M.; Morhange, J.F.; Julien, C.; Diamant, R.; Fernández-Guasti, M.; Fuentes, G.A.; Alonso, J.C. Micro-Raman characterization of WO₃ and MoO₃ thin films obtained by pulsed laser irradiation. *Appl. Surf. Sci.* **1998**, *127–129*, 674–678. [[CrossRef](#)]
25. Chai, Y.; Tam, C.W.; Beh, K.P.; Yam, F.K.; Hassan, Z. Effects of thermal treatment on the anodic growth of tungsten oxide films. *Thin Solid Films* **2015**, *588*, 44–49. [[CrossRef](#)]
26. Badot, J.C.; Beluze, L.; Dubrunfaut, O. Particle size effect on the electronic conductivity of electroactive Li_xWO₃-H₂O powders: A study from 10³ to 10¹⁰ Hz. *J. Phys. Chem. C* **2009**, *112*, 14549–14554. [[CrossRef](#)]
27. Faughnan, B.W.; Crandall, R.S.; Lampert, M.A. Model for the bleaching of WO₃ electrochromic films by an electric field. *Appl. Phys. Lett.* **1975**, *27*, 275–277. [[CrossRef](#)]

28. Srivastava, A.K.; Deepa, M.; Singh, S.; Kishore, R.; Agnihotry, S.A. Microstructural and electrochromic characteristics of electrodeposited and annealed WO₃ films. *Solid State Ion.* **2005**, *176*, 1161–1168. [[CrossRef](#)]
29. Koo, B.R.; Ahn, H.J. Fast-switching electrochromic properties of mesoporous WO₃ films with oxygen vacancy defects. *Nanoscale* **2017**, *9*, 17788–17793. [[CrossRef](#)] [[PubMed](#)]



© 2018 by the authors. Licensee MDPI, Basel, Switzerland. This article is an open access article distributed under the terms and conditions of the Creative Commons Attribution (CC BY) license (<http://creativecommons.org/licenses/by/4.0/>).